Proceedings of the ASME 2007 International Design Engineering Technical Conferences & Computers and Information in Engineering Conference
IDETC/CIE 2007
September 4-7, 2007, Las Vegas, Nevada, USA

DETC2007-34471

SYNTHESIS OF THE BODY SWING ROTATOR JOINT ALIGNING MECHANISM FOR THE ABDUCTOR JOINT OF A NOVEL TRIPEDAL LOCOMOTION ROBOT

Dennis W. Hong*
RoMeLa: Robotics & Mechanisms Lab
Mechanical Engineering Department
Virginia Polytechnic Institute and State University
Blacksburg, Virginia 24061
Email: dhong@vt.edu

Derek F. Lahr
RoMeLa: Robotics & Mechanisms Lab
Mechanical Engineering Department
Virginia Polytechnic Institute and State University
Blacksburg, Virginia 24061
Email: dlahr@vt.edu

ABSTRACT

The unique three-legged walking robot STriDER (Self-excited Tripedal Dynamic Experimental Robot) utilizes a novel tripedal gait which incorporates aspects of passive dynamic walking into a stable tripedal platform to walk efficiently, and is also capable of changing directions. This unique tripedal gait, however, requires three abductor joints to align two of the three body swing rotator joints in the body, depending on the direction of the step the robot takes. In an earlier prototype of STriDER, the three abductor joints were independently actuated using three DC motors to align the rotator joints which made the robot heavy and inefficient.

In this paper, we present the synthesis, analysis, and mechanical design of a novel mechanism for actuating the three abductor joints of this unique three-legged walking robot to generate the required motion using only a single actuator. The mechanism utilizes an internal gear set to generate a Hypotrochoid path curve and uses pin-in-slot joints to coordinate the motion of the three abductor joints to guide them through the four sets of positions required to enable the robot to walk efficiently.

A brief description and background of the tripedal locomotion robot STriDER is presented first, followed by the design constraints and requirements of the abductor joint mechanism. Synthesis and kinematic analysis of the mechanism is presented with a study of the force transmission characteristics for a quasi-static case. A description of the detailed mechanical design, results from the experiments, and a conclusion with a discussion for future work is presented next.

1. INTRODUCTION

STriDER (Self-excited Tripedal Dynamic Experimental Robot) [1 to 5] is a unique walking machine with three legs that utilizes a novel tripedal gait. The robot has three abductor joints, whose axis of rotation are perpendicular to the robot base, which are used to align two of the three body swing rotator joints depending on the direction of the robot's step. In an earlier prototype of STriDER, the three abductor joints were independently actuated using three DC motors to align the rotator joints which made the robot heavy and inefficient. The required coordinated motion of the legs though only requires one degree of freedom and therefore only one actuator with an appropriate mechanism.

This paper presents a novel rotator joint aligning mechanism for STriDER. The synthesis, analysis, and mechanical design of a novel mechanism for actuating the three abductor joints of this unique three-legged walking robot will be presented. Two mechanisms were initially considered for such an application. The first used a simple pin mounted upon a rotating arm to actuate the abductor through several slots. The mechanism finally chosen utilizes an internal gear set to generate a Hypotrochoid path curve and uses pin-in-slot joints to coordinate the motion of the three abductor joints to guide them through the four sets of positions required to enable the robot to walk efficiently. Three of these positions are those in which two of the three rotator joints are aligned, and the fourth position is the neutral position in which all three rotator joint axis intersect at the center of the robot.

A brief description and background of the tripedal locomotion robot STriDER is presented first, followed by the design constraints and requirements of the abductor joint

*Address all correspondence to this author.

mechanism. Synthesis and kinematic analysis of the mechanism is presented with a study of the force transmission characteristics for a quasi-static case, which confirms the initial hypothesis that several points of infinite mechanical advantage exist. The detailed mechanical design, experimental results, and a discussion for future work are also described.

2. BACKGROUND

2.1 STriDER (Self-excited Tripedal Dynamic Experimental Robot

STriDER is a novel three-legged walking machine (Fig. 1) that exploits the concept of actuated passive dynamic locomotion [1 to 5], to dynamically walk with high energy efficiency and minimal control using its unique tripedal gait as shown in Fig. 2 (patent pending). Unlike other passive dynamic walking machines, this unique tripedal locomotion robot is inherently stable with its tripod stance, can change directions, and is relatively easy to implement, making it practical to be used for real life applications (a video of it walking is presented in [3]). Thus, the proper mechanical design of a robot can provide energy efficient locomotion without sophisticated control methods [6].

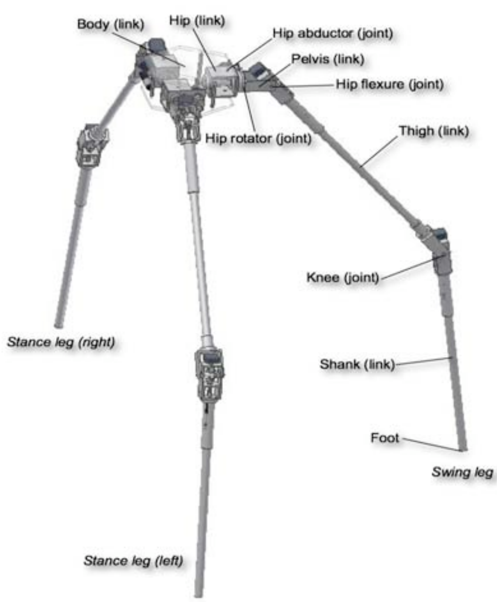

Figure 1. Joint and link names for the first prototype of STriDER [2].

Fig. 2 shows the concept of the single step tripedal gait. From its starting position (Fig. 2 (a)), as the robot shifts its center of gravity by aligning two of its pelvis links (thus aligning the hip rotator joints) using the hip abductor joints (Fig. 2 (b)), the body of the robot can fall over in the direction perpendicular to the line connecting the two feet of the stance legs (Fig. 2 (c)). As the robot falls over, the leg in the middle (swing leg) naturally swings between the two stance legs (Fig. 2 (d)) and catches the fall (Fig. 2 (e)). As all three legs contact the ground, the robot resets its posture by actuating its joints, storing potential energy for its next gait (Fig. 2 (f)). The key to this tripedal gait is the natural swinging motion of the swing leg, and the flipping of the body about the aligned hip rotator joints connecting the two stance legs. With the appropriate mechanical design parameters (mass properties and dimension of the links) [2, 4], this motion is repeated with minimal control and power consumption by exploiting its built in dynamics.

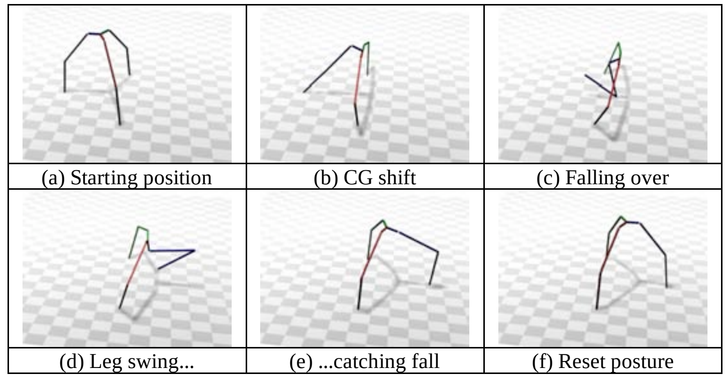

Figure 2. Single step tripedal gait.

The walking path, shown in Figure 3, illustrates how the STriDER walks straight and how it can change directions. The changing of direction is done through a unique sequencing of the choice of the swing leg among the three (patent pending). By altering the stride width and the direction of the swing, a variety of different paths can be formed.

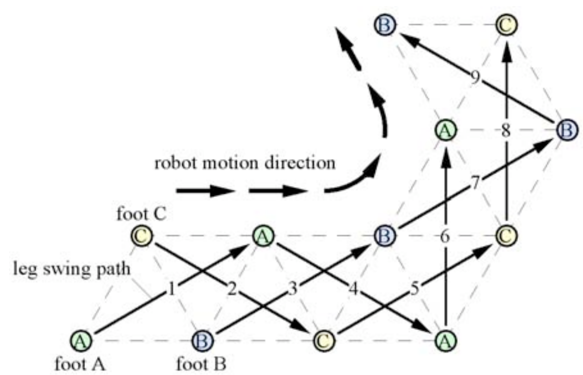

Figure 3. Gait strategies for changing directions.

The simple tripod configuration and tripedal gait of STriDER has many advantages over other legged robots; it has a simple kinematic structure (vs. quadrupeds, hexapods, or humanoid bipeds) that prevents conflicts among its legs and between its legs and the body; it is inherently stable (like a camera tripod); it is simple to control (vs. bipeds) as it is a simple falling motion in a predetermined direction and catching its fall; it is energy efficient, exploiting the actuated passive dynamic locomotion concept utilizing its built in dynamics; it is lightweight enabling it to be launched to difficult to access areas; and it is tall which makes it ideal for deploying and positioning sensors at high positions for surveillance.

The design of the first prototype with optimized design parameters (link lengths, mass properties, location of center of mass for each link, etc.) for a smooth gait, and the resulting simple experiments (Fig. 4) for a single step tripedal gait are presented in [4]. Dynamic modeling, simulation, and motion generation strategies using the concept of self-excitation is presented in [2]. The inverse and forward displacement analysis of the pose of STriDER when all three feet are on the ground is presented in [5].

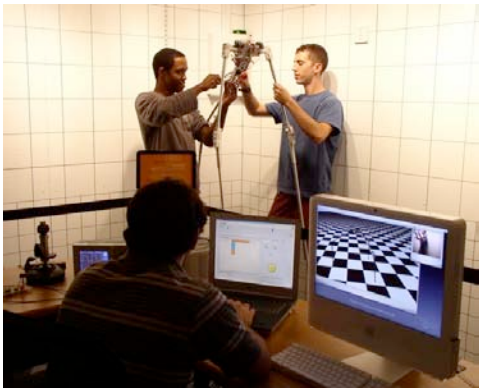

Figure 4. Experiment setup for a single step tripedal gait.

2.2 Abductor Joint

The tripedal gait requires the entire body of STriDER to rotate about the two hip rotator joints of the stance legs as the swing leg swings between them. Since any one of the three legs can be chosen as the swing leg, any two of the three hip rotator joints need to be able to align to each other. The hip abductor joints perform this motion by changing the angle of the hip rotator joints so that the axis of one hip rotator joint can be aligned to another while the third is set to be perpendicular to this axis.

In the first prototype of STriDER [2, 4] as shown in Figure 4, the three hip abductor joints were independently actuated and controlled with three separate DC motors. While this approach worked, the size and weight of the two additional motors made the design undesirable, as it essentially requires only a single degree of freedom motion for a successful operation of aligning the rotator joints. This is the motivation behind the work presented in this paper. The following describes the analysis, synthesis, and design of a single degree of freedom hip abductor joint mechanism that will successfully align any two of the three hip rotator joints with a single input from a DC motor.

3. SYNTHESIS OF THE ABDUCTOR JOINT MECHANISM

3.1 Abductor Joint Mechanism for Three Output Positions

For STriDER to successfully perform the tripedal gait, the motion of the three abductor joints need to be coordinated such that any two of the three hip rotator joints can be aligned. Thus the new single degree of freedom abductor joint mechanism must allow the three abductor joints to go through three specific joint positions each as the single input link rotates one full revolution.

The first abductor joint mechanism concept uses three slotted abductor locator links (Figure 5, 6) where a pin on the positioning arm slides inside these slots. As the positioning arm rotates about the center, the pin in slot joint constrains the abductor locator links' motion. With the appropriate dimensions, this mechanism will allow the three abductor joints to go through the three specific joint positions to allow the hip rotator joints to be aligned properly as shown in Figure 5, note that the triangular base remains stationary while the positioning arm rotates.

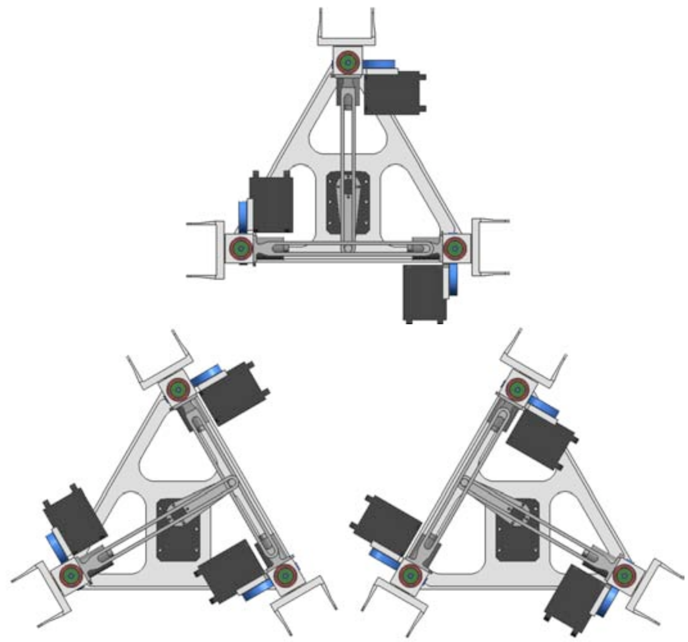

Figure 5. The three positions of the rotator joint aligning mechanism.

For the dimensional synthesis, a displacement analysis is performed for this mechanism. Figure 6 shows this mechanism and the vectors defined for a single abductor joint.

For the three abductor locator links to go through the specified positions and be synchronized, the length of the positioning arm (r_2) must be half of the distance between the abductor joint (O_4) and the center of the body (O_2) thus

$$r_2 = \frac{r_1}{2} \tag{1}$$

and the angle θ_1 that defines the location of the abductor joint (O_4) is

$$\theta_1 = -\frac{\pi}{6} \tag{2}$$

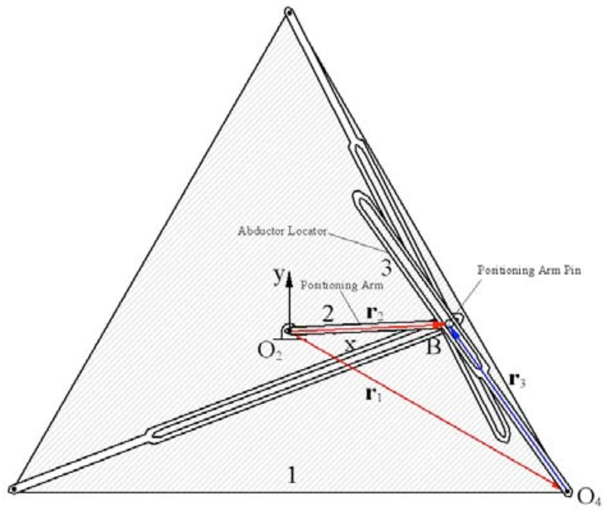

Figure 6. Vectors defined for the rotator joint aligning mechanism with three positions.

From this, a displacement analysis can be performed using simple trigonometry. With the angular position of the positioning arm (θ_2) as the input, the angular position of the abductor locator link (θ_3) can be expressed as

$$\theta_3 = \frac{5\pi}{6} - a\tan 2\left(2 - Cos(\theta_2 + \frac{\pi}{6}), Sin(\theta_2 + \frac{\pi}{6})\right) \tag{3}$$

and the position of the positioning arm pin in the abductor locator slot (r_3) can be expressed as

$$r_3 = \sqrt{5r_2^2 - 4r_2^2 Cos(\theta_2 + \frac{\pi}{6})} \tag{4}$$

Figure 7 shows the angular position of the abductor locator link (θ_3) as a function of the positing arm (θ_2). As expected, it oscillates between the two extreme positions $2\pi/3$ and π.

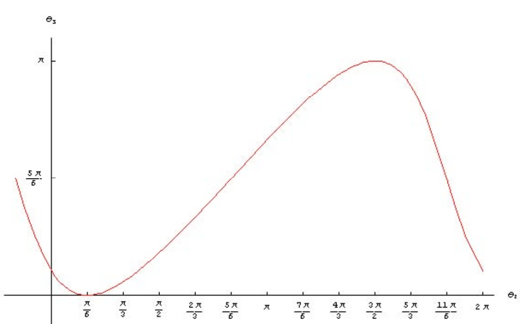

Figure 7. Angular position of the abductor locator link (θ_3) against the input angle (θ_2).

To verify that the three abductor locator links move in synchronous motion and reach the three specified positions in order to align the two of the three hip rotator joints, the angular positions of all three abductor locator links (θ_{3a}, θ_{3b}, θ_{3c}) are plotted together against the angular input position of the positing arm (θ_2) as shown in Figure 8. As expected, two of the three abductor locator links align the rotator joints in sequence at $\pi/6$, $5\pi/6$, and $3\pi/2$ of the positioning arm as it goes through one full revolution.

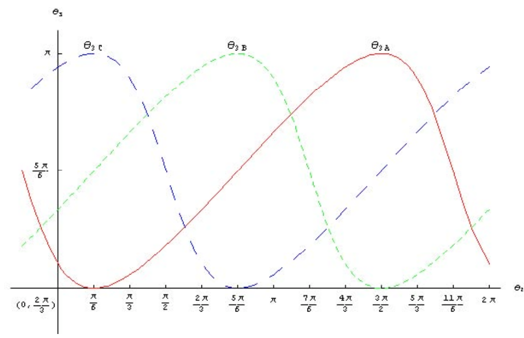

Figure 8. Angular position of all three abductor locator links (θ_{3a}, θ_{3b}, θ_{3c}) against the input angle (θ_2).

To figure out the required length of the abductor locator link and the length required for the slot, the positioning arm pin location in the abductor locator slot (r_3) is plotted against the input position of the positoining arm (θ_2) for one full revolution as shown in Figure 9.

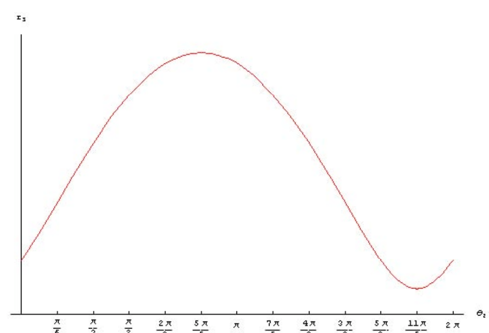

Figure 9. Location of the pin in the abductor locator link slot (r_3) against the input angle (θ_2).

The maximum value of r_3 is 15.24cm when θ_2 is $5\pi/6$, and the minimum value of r_3 is 5.08cm when θ_2 is $11\pi/6$. From this, we can find that the total stroke, or the required length of the slot (Δr_3) should be at least 10.16cm and the length of the abductor locator link at least 15.24cm.

3.2 Abductor Joint Mechanism for Four Output Positions

The synthesized rotator joint aligning mechanism above does satisfy the minimum requirements of achieving the three position configurations of aligning two of the three pelvis links for taking steps in the three corresponding directions. However, it is desirable for the mechanism to enable an additional position configuration of the three pelvis links to be positioned equally spaced, 120° a part. This is useful as STriDER's default position when it is not taking a step.

Using the given general mechanical structure with the three slotted abductor locator links, in order to achieve this additional position configuration, the pin of the positioning arm needs to reach the center of the body (O_2) as well. This can be achieved by utilizing an internal gear set to generate a hypotrochoid path curve [7] (Figure 10) for the pin of the positioning arm. A hypotrochoid is a roulette traced by a point attached to a circle rolling around the inside of a fixed circle.

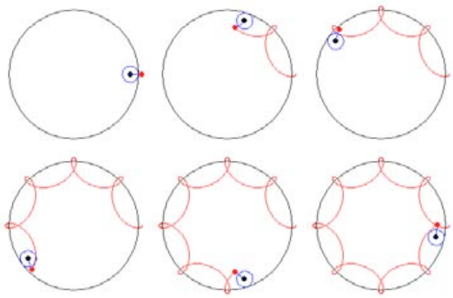

Figure 10. A hypotrochoid curve.

By choosing the appropriate diameters of the gears and dimensions of the links, a mechanism can be synthesized such that with only a single input rotation of the carrier link, the pin of the positioning arm can trace a path to reach not only the three required positions for aligning the pelvis links, but also position them in the additional neutral center position. For the positioning arm pin to reach the 4 required positions, it must trace a special kind of hypotrochoid curve called the trifolium [7]. Trifolium is the three-lobed folium also known as the 3-petalled rose as shown in Figure 11.

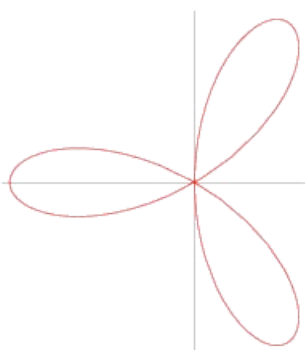

Figure 11. A hypotrochoid trifolium curve.

If the path of the pin can follow a trifolium curve, the mechanism can guide the hip rotator joint through the four specific positions, is shown in Figure 12.

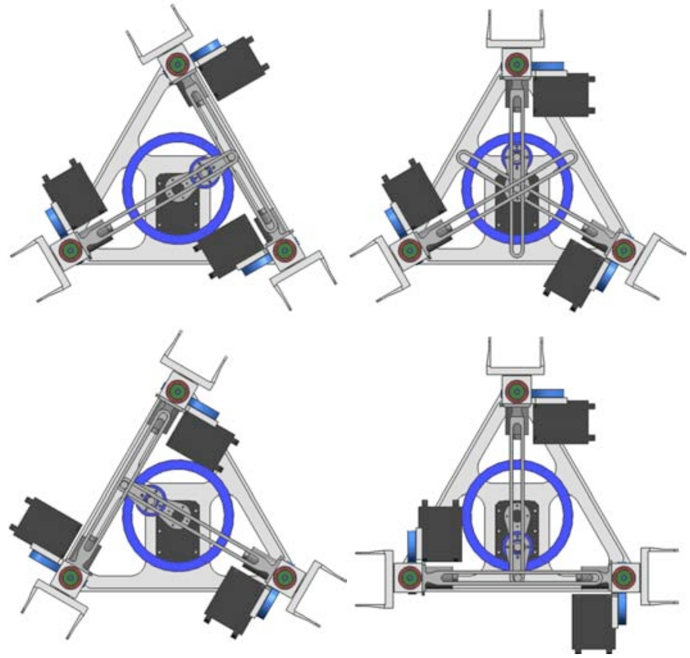

Figure 12. The four positions of the rotator joint aligning mechanism with internal gear set.

Geometric Constraints and the Position Solution

To synthesize this mechanism, the geometric constraints were first derived. Figure 13 shows this mechanism and the vectors defined for a single abductor joint. There would be two more identical mechanisms that share the same positioning arm pin.

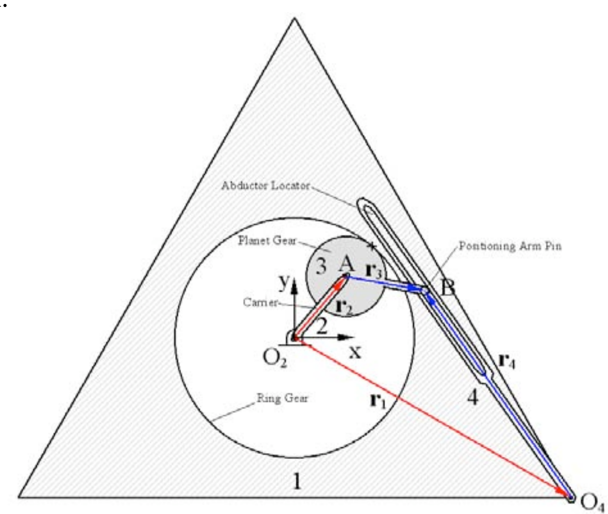

Figure 13. Vectors defined for the rotator joint aligning mechanism with four positions.

To generate trifolium path of the pin as shown in Figure 14, first, the radii ratio between the external ring gear and the internal gear must be 3:1, thus,

$$\rho_1 = 3\rho_3 \tag{5}$$

This defines the length of the carrier link (r_2) as

$$r_2 = \rho_1 - \rho_3 \tag{6}$$

Additionally, since the pin of the positioning arm must pass the center, the length of the carrier link (r_2) and the positioning arm (r_3) must be equal as

$$r_3 = r_2 \tag{7}$$

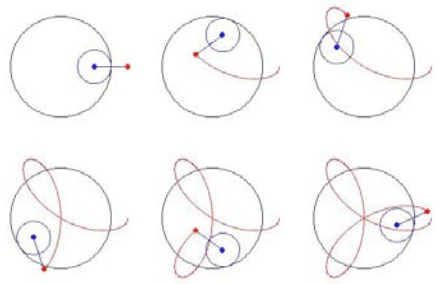

Figure 14. The path of the trifolium curve goes through the three extreme positions and the center position.

For the abductor locator links to align properly and to move within their allowable 60° range of motion, the abductor bearing (O_4) is positioned such that the length of the vector defining its position is constrained as

$$r_1 = 2(r_2 + r_3) \tag{8}$$

and it's angle as

$$\theta_1 = -\frac{\pi}{6} \tag{9}$$

Since rolling contact exists between the ring gear and internal planet gear, the angular position between the input carrier link (θ_2) and the positioning arm (θ_3) is constrained by

$$\theta_3 = \frac{\pi}{2} + (1 - \frac{\rho_1}{\rho_3})\theta_2 \tag{10}$$

To find the position solution of the links and to figure out the displacement length of the pin inside the abductor locator slot, the vectors defined in Figure 13 must satisfy the loop-closure equation

$$\mathbf{r}_2 + \mathbf{r}_3 - \mathbf{r}_4 - \mathbf{r}_1 = 0 \tag{11}$$

The two corresponding scalar equations for the x and y components of this vector equation are

$$r_2 \cos\theta_2 + r_3 \cos\theta_3 - r_4 \cos\theta_4 - r_1 \cos\theta_1 = 0 \tag{12}$$
$$r_2 \sin\theta_2 + r_3 \sin\theta_3 - r_4 \sin\theta_4 - r_1 \sin\theta_1 = 0 \tag{13}$$

where the two unknown variables, the angular position of the abductor locator link (θ_4) and the position of the positioning arm pin in the abductor locator slot (r_4) can be solved for.

By dividing Equation (13) by Equation (12), the angular position of the abductor locator link (θ_4) can be expressed as

$$\theta_4 = a\tan 2(\cos\theta_2 + \cos\left[\frac{\pi}{2} - 2\theta_2\right] - 4\cos\theta_1, \sin\theta_2 + \sin\left[\frac{\pi}{2} - 2\theta_2\right] - 4\sin\theta_1) \tag{14}$$

By adding the square of Equations (12) and (13) we have:

$$r^2{}_4 = r_1^{\,2} + r_2^{\,2} + r_3^{\,2} - 2r_1r_2\cos(\theta_1 - \theta_2) + 2r_2r_3\cos(\theta_2 - \theta_3) - 2r_1r_3\cos(\theta_1 - \theta_3) \tag{15}$$

Using the constraints between r_1, r_2, and r_3 by applying Equations (7) and (8) to Equation (15) results in:

$$r^2{}_4 = 18r_2^{\,2} - 8r_2^2\cos(\theta_1 - \theta_2) + 2r_2^2\cos(\theta_2 - \theta_3) - 8r_2^2\cos(\theta_1 - \theta_3) \tag{16}$$

Applying the trigonometric addition formulas and substituting θ_1 and θ_3 using Equations (9) and (10) yields

$$r^2{}_4 = 18r_2^{\,2} - 8r_2^2\cos(-\theta_2 - \frac{\pi}{6}) + 2r_2^2\cos(3\theta_2 - \frac{\pi}{2}) - 8r_2^2\cos(2\theta_2 - \frac{2\pi}{3}) \tag{17}$$

Finally, the position of the positioning arm pin in the abductor locator slot (r_4) can be expressed as

$$r_4 = r_2\sqrt{18 - 8\cos(-\theta_2 - \frac{\pi}{6}) + 2\cos(3\theta_2 - \frac{\pi}{2}) - 8\cos(2\theta_2 - \frac{2\pi}{3})} \tag{18}$$

Figure 15 shows the angular position of the abductor locator link (θ_4) as a function of the input carrier link (θ_2). As expected, it oscillates between the two extreme positions $2\pi/3$ and π.

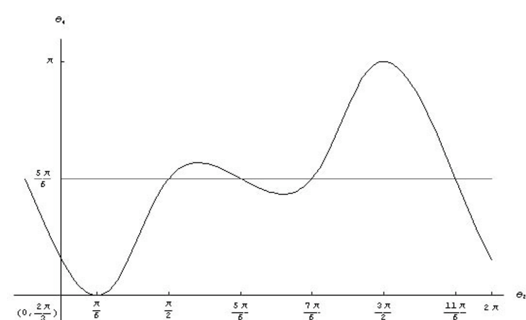

Figure 15. Angular position of the abductor locator link (θ_4) against the input angle (θ_2).

To verify that the three abductor locator links move in synchronous motion and reach the four specified positions in order to align the two of the three hip rotator joints and reach the neutral position, the angular positions of all three abductor locator links (θ_{4a}, θ_{4b}, θ_{4c}) are plotted together against the angular input position of the input carrier link (θ_2) as shown in Figure 16. As expected, two of the three abductor locator links align the rotator joins in sequence at $\pi/6$, $5\pi/6$, and $3\pi/2$, and all three reach the neutral position at $\pi/2$, $7\pi/6$, and $11\pi/6$ of the input carrier link as it goes through one full revolution.

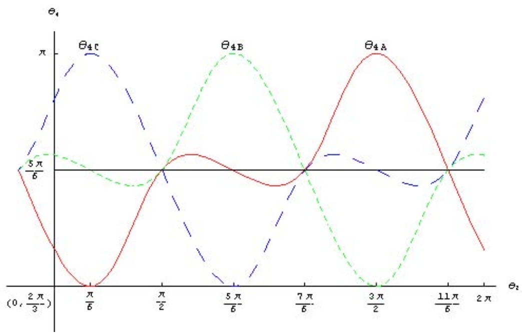

Figure 16. Angular position of all three abductor locator links (θ_{4a}, θ_{4b}, θ_{4c}) against the input angle (θ_2).

To figure out the required length of the abductor locator link and the length required for the slot, the positioning arm pin location in the abductor locator slot (r_4) is plotted against the input position of the input carrier link (θ_2) for one full revolution as shown in Figure 17. The length of r_1 is set as 10.16cm.

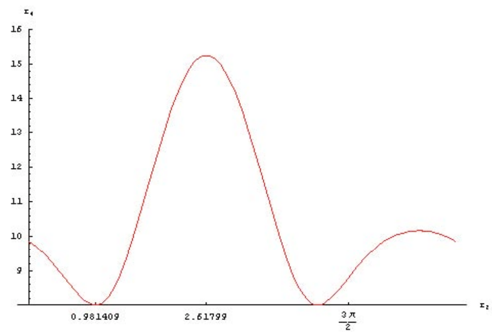

Figure 17. Location of the pin in the abductor locator link slot (r_4) against the input angle (θ_2).

To find when the maximum and minimum distance of the positioning arm pin location in the abductor locator slot (r_4) occurs, Equation (18) is differentiated with respect to the input carrier link (θ_2) as

$$\frac{dr_4}{d\theta_2} = \frac{r_2\left[3\cos 3\theta_2 - 8\sin(\frac{2\pi}{3} - 2\theta_2) + 4\sin(\frac{\pi}{6} + \theta_2)\right]}{\sqrt{9 + \sin 3\theta_2 - 4\cos(\frac{2\pi}{3} - 2\theta_2) - 4\cos(\frac{\pi}{6} + \theta_2)}} \tag{19}$$

Setting this to 0 shows that the maximum value of r_4 is 15.24cm when θ_2 is $5\pi/6$, and the minimum value of r_3 is 8.01cm when θ_2 is 0.981 [rad]. From this, we can find that the total stroke, or the required length of the slot (Δr_4) should be at least 7.23cm and the length of the abductor locator link at least 15.24cm.

4. ANALYSIS OF THE ABDUCTOR JOINT MECHANISM

4.1 Kinematic Analysis and Input Actuation

The successful synthesis of the four position abductor joint mechanism was verified by the displacement kinematic analysis above. Next, to see the velocity relationship between the input angular velocity (ω_2) and the output angular velocities (ω_4 for each abductor locator link), we use the method of kinematic coefficients [8] which provides useful geometric insight into the motion of the linkage.

Differentiating the two scalar equations for the x and y components of the vector closure equation, Equations (12) and (13), with respect to the input variable θ_2 (rather than with respect to time)

$$\begin{aligned} -r_2\sin\theta_2 - r_3\sin\theta_3\theta_3' - r_4'\cos\theta_4 + r_4\sin\theta_4\theta_4' &= 0 \\ r_2\cos\theta_2 + r_3\cos\theta_3\theta_3' - r_4'\sin\theta_4 - r_4\cos\theta_4\theta_4' &= 0 \end{aligned} \tag{20}$$

where θ'_3 r'_4 and θ'_4 are the first order kinematic coefficients for the angle of link 3, length and angle of link 4, respectively, and defined as

$$\theta_3' = \frac{d\theta_3}{d\theta_2} \tag{21}$$

$$r_4' = \frac{dr_4}{d\theta_2} \tag{22}$$

$$\theta_4' = \frac{d\theta_4}{d\theta_2} \tag{23}$$

From the relationship between the input angle and the angle of link 3, Equation (10), and by differentiating it with respect to the input variable θ_2, the first order kinematic coefficients for the angle of link 3 can be found as

$$\theta_3' = 1 - \frac{\rho_1}{\rho_3} \tag{24}$$

Substituting this into Equation (20), we can solve for the first order kinematic coefficients for the length and angle of link 4 from the linear set of equations

$$\begin{bmatrix} r_4\sin\theta_4 & -\cos\theta_4 \\ -r_4\cos\theta_4 & -\sin\theta_4 \end{bmatrix}\begin{Bmatrix} \theta_4' \\ r_4' \end{Bmatrix} = \begin{Bmatrix} r_2\sin\theta_2 + r_3\sin\theta_3\left(1 - \frac{\rho_1}{\rho_3}\right) \\ -r_2\cos\theta_2 - r_3\cos\theta_3\left(1 - \frac{\rho_1}{\rho_3}\right) \end{Bmatrix} \tag{25}$$

The first order kinematic coefficients for both length and angle of link 4 for a full revolution of the input θ_2 is shown in the plots (Figures 18, 19).

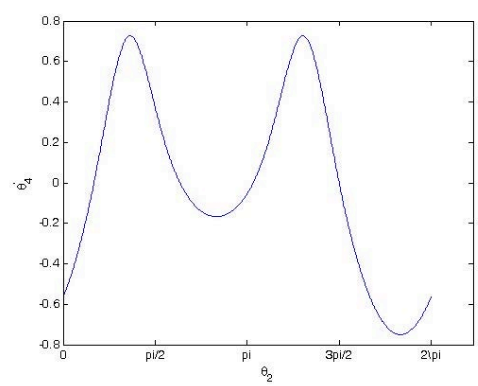

Figure 18. The first order kinematic coefficients for the angle (θ_4) of link 4 for a full rotation of input angle (θ_2).

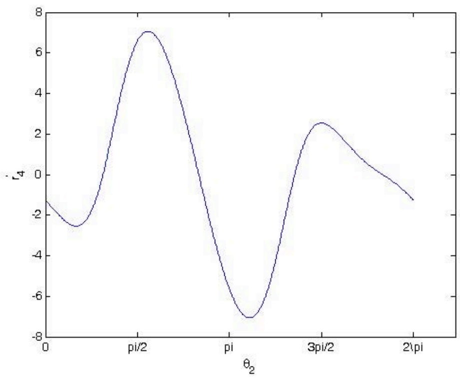

Figure 19. The first order kinematic coefficients for the length (r_4) of link 4 for a full rotation of the input angle (θ_2).

Then the velocities for the links can be found by multiplying their first order kinematic coefficients by the input velocity ω_2 as

$$\omega_4 = \theta_4' \omega_2 \tag{26}$$
$$\omega_3 = \theta_3' \omega_2 \tag{27}$$
$$v_4 = r_4' \omega_2 \tag{28}$$

4.2 Quai-static Force Analysis and Force Transmission Characteristics

Quasi-static Force Analysis

Though the dynamic effects of the novel tripedal gait are a key to the general locomotion strategy of STriDER, the motion of aligning of the pelvic links does not contribute to this as this motion is not performed during the falling or swinging phase. Thus no acceleration analysis is performed and only the quasi-static force analysis is performed to check the force transmission characteristics of the synthesized mechanism.

It order to find a capable abductor actuator, it is necessary to find the relationship between the input torque on the abductor joint, and the output torque on the abductor locator link for any carrier position. For the quasi-static case, a free body diagram was drawn for the carrier, positioning arm, and the abductor locator links. The forces on the carrier are defined as seen in Figure 20, where F_{12} is the reaction force of the carrier on the motor, F_{32} is the reaction force of the planet gear on the carrier, and τ_2 is the input motor torque. Summing the moments about O_2 yields Equation 29:

$$\tau_2 + F_{32} \cdot r_2 Cos(\theta_2) \cdot Sin(\theta_{32}) - F_{32} \cdot r_2 Sin(\theta_2) \cdot Cos(\theta_{32}) = 0 \cdot \tag{29}$$

A free body diagram of the abductor positioning arm and planet gear assembly shows the reaction force from the ring gear, F_{r3}; the reaction force on the pin from the locator arm, F_{43}; and the bearing reaction force, F_{32}. The forces in Figure 21 are summed in the x and y-direction, and the moments are taken about point *A* to yield Equations 30 through 32. In the x-direction, the result is:

$$F_{r3} \cdot Sin(\theta_2) - F_{32} \cdot Sin(\theta_{32}) \cdot - F_{43} \cdot Sin(\theta_4) = 0 \tag{30}$$

In the y-direction this yields:

$$-F_{r3} \cdot Cos(\theta_2) + F_{32} \cdot Sin(\theta_{32}) \cdot + F_{43} \cdot Cos(\theta_4) = 0 \tag{31}$$

and finally summing the moments about *A* yields:

$$-F_{r3} \cdot \rho_3 + F_{43} \cdot r_3 \cdot Cos(\theta_3) \cdot Cos(\theta_4) + F_{43} \cdot r_3 \cdot Sin(\theta_3) \cdot Sin(\theta_4) = 0 \tag{32}$$

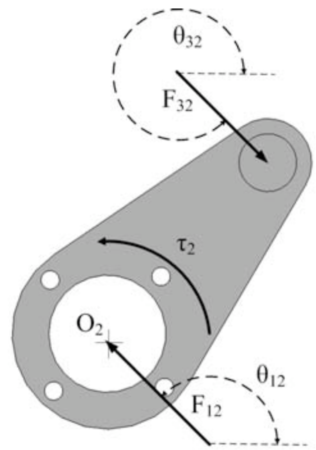

Figure 20. Free body diagram of the carrier showing the motor torque τ_2.

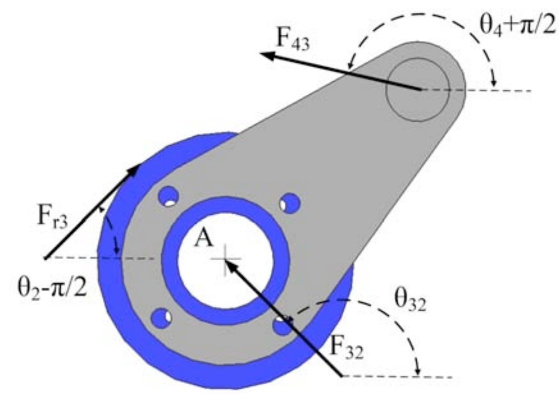

Figure 21. Free body diagram of the planet gear and abductor positioning arm assembly.

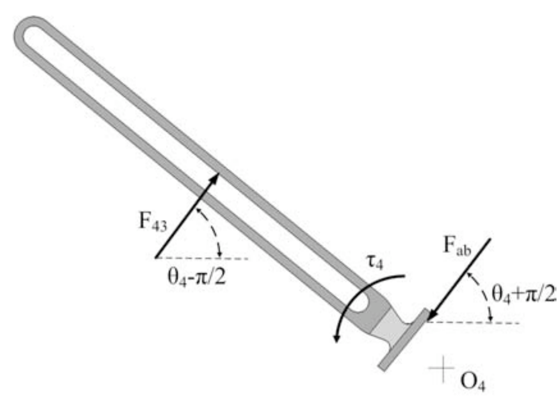

Figure 22. Free body diagram of the abductor locator arm.

Summing the moments on the abductor locator arm about point O_4, seen in Figure 22, will yield Equation 33:

$$\tau_4 - F_{43} \cdot r_4 = 0 \tag{33}$$

Forming a system of Equations 29 through 33 and solving for τ_2 in terms of the knowns, θ_2, θ_3, θ_4, r_2, r_3, r_4, ρ_3 and τ_4, will result in Equation 34:

$$\tau_2 = \tau_4 \cdot \left(\frac{r_2 \rho_3 Cos(\theta_2 - \theta_4) - r_2 r_3 Cos(\theta_3 - \theta_4)}{r_4 \rho_3} \right) \tag{34}$$

which can be used to find the mechanical advantage of the abductor joint mechanism.

The mechanical advantage and efficiency are used to observe the force transmission characteristics and energy loss of the mechanism over its range of motion. In this section, we define mechanical advantage for the rotator aligning mechanism and observe how it changes over one revolution of the carrier.

We can use Equation 6 to find the mechanical advantage, τ_4/τ_2, given arbitrary values of r_4, θ_2, θ_3, and θ_4. This can be seen in Equation 35:

$$\frac{\tau_4}{\tau_2} = \cdot \left(\frac{r_4 \rho_3}{r_2 \rho_3 Cos(\theta_2 - \theta_4) - r_2 r_3 Cos(\theta_3 - \theta_4)} \right) \tag{35}$$

To incorporate the other constraints of the system, Equations 10, 14 and 18 were used with Equation 7 to find the mechanical advantage for a range of values of θ_2. The mechanical advantage for a full rotation of the carrier can be seen in Figure 23 for one abductor. There are four points of infinite mechanical advantage, two of which correspond to the aligned positions of two adjacent rotator joints. Thus for the swing phase of the walking gait, no force from the abductor joints is transferred to the motor. This behavior allows the abductor joint to be self-locking in these positions and lowers the torque requirements of the motor.

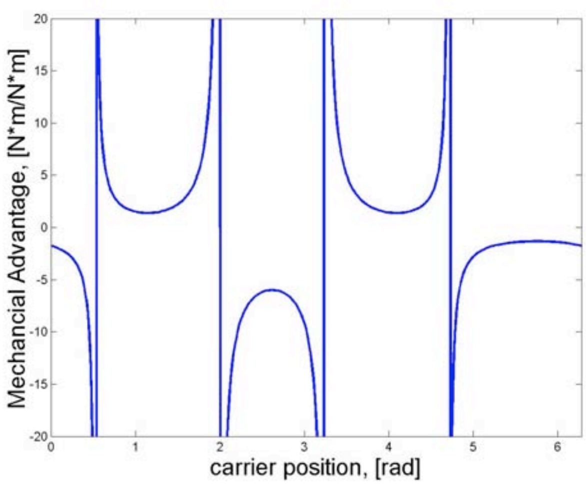

Figure 23. Mechanical advantage of the aligning mechanism actuator versus the abductor locator arm.

5. MECHANICAL DESIGN AND EXPERIMENTS

A prototype was built to validate the operating principles and performance of STriDER and the Rotator Joint Aligning mechanism.

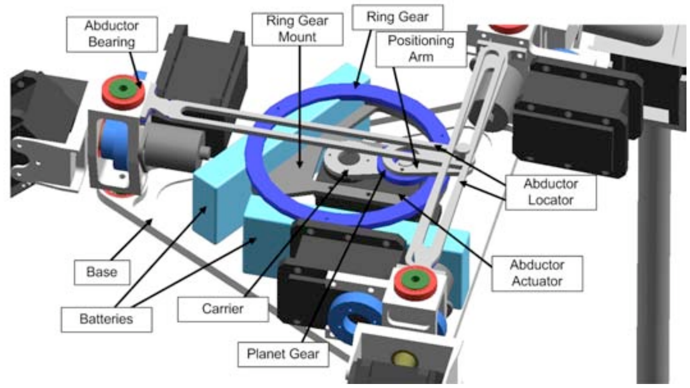

Figure 24. Mechanical design of STriDER showing the individual component names.

5.1 Mechanical Design

The robot stands roughly .75[m] tall with a body that is approximately 18[cm] across the triangular base. Nearly all components aside from gears and bearings were CNC machined from 6061 aluminum. All joints are supported on ball bearings to reduce friction from the large moments produced by the legs. The gears of the planetary gearset are also made of aluminum; the ring gear having a 7.62[cm] pitch diameter, and the planet gear a 2.54[cm] pitch diameter for the required 3:1 actuation ratio. This planet gear is supported by a miniature ball bearing on the carrier. This ring gear size was chosen to be the smallest diameter possible while preventing any interference between itself and the rotator actuator. The planetary gearset is actuated by a Robotis RX-28 intelligent servo motor as are the rotator joints. Utilizing the building block structure of these motors, the abductor actuator also serves as the ring gear support through the ring gear mount which increases the rigidity and reduces error in the system, as seen in Figure 25. Both the flexor and knee joint are currently actuated with the Robotis DX-24 servos.

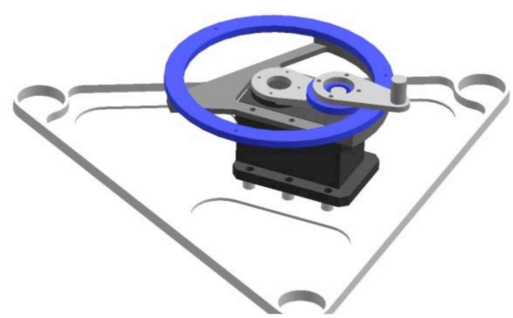

Figure 25. Direct attachment of the ring gear to the motor for increased system rigidity and accuracy

The control arm fixed to the planer gear and its associated post are machined from one piece of aluminum for increased rigidity and reduced size. There is a slip fit between the post and the slots of the abductor locator arms to minimize any play in the abductor joint. As such, in the physical prototype, virtually no play can be felt in the movement of the abductor. Currently this pin and slot joint utilizes sliding of like materials, aluminum on aluminum, and thus wear and friction could become problematic. At this point though the joint does not inhibit the operation of the mechanism in any way. Future prototypes will integrate a suitable bushing surface between the pin and slots. A certain amount of compliance is built into the abductor locator arms via a narrow cross section to reduce any shock loading of the mechanism. These arms are bolted to the rotator link for ease of replacement in case of redesign and for interchangeability of parts. Stress concentrations are minimized here through the use of radiused corners as seen in Figure 26.

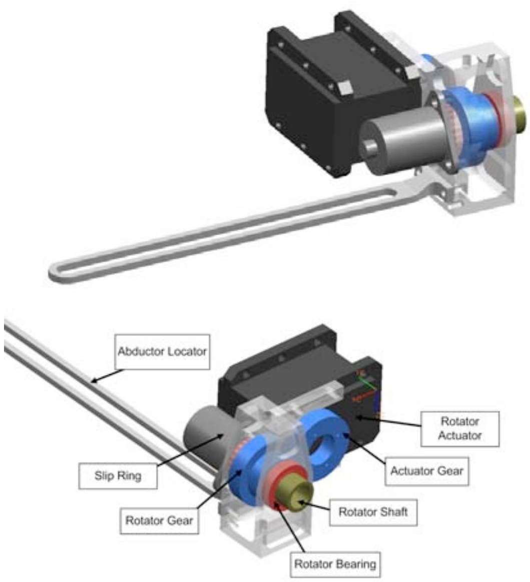

Figure 26. Abductor Locator Arms and Rotator assembly showing the slip rings and modular design.

Because of the continuous inverting motion inherent to the locomotion strategy of this robot, slip rings were built into the rotator joint, which can be seen in Figure 2. It was necessary then to remove the actuator away from the rotation axis of the joint such that wires could be routed through the rotator shaft. Therefore this joint is actuated through a 1:1 spur gear system with a 25.4[mm] pitch diameter. The rotator gear is then pinned to the rotator shaft for easy component assembly. This particular motor configuration was chosen as a balance between the overall body size and the abductor to flexor joint separation distance. In this position, the separation of the flexor and abductor joint is minimized to 40[mm] without enlarging the body by a considerable amount due to interference issues between the ring gear and rotator actuator. The legs are fairly straightforward; the flexor link is pressed onto the rotator shaft which is attached to the thigh link through a collar. A similar design is also utilized for the knee joint. A complete model can be seen next to the actual prototype in Figure 27

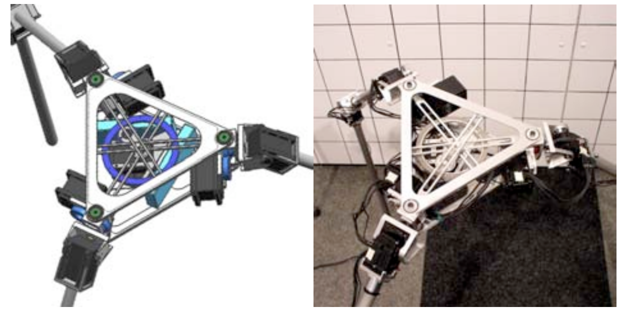

Figure 27. The CAD model (left) and the actual prototype (right) of the rotator joint aligning mechanism

5.2 Tests and Prototype Evaluation

Both the original prototype of STriDER and the new version using the presented mechanism is shown in Figure 28. Upon final assembly, the robot was able to support itself and cycle through the four positions required of the rotator joint aligning mechanism. Each pair of joints lines up properly, and in between these positions, the mechanism cycles through the stance position, when all rotator joint axes intersect in the middle. Due to slight manufacturing errors, there is a small amount of backlash in the ring/planet gear connection, but this has little effect on the abductor actuation. The motion of the mechanism is smooth and predictable while running free of lubrication. There is no apparent binding due to poor force transmission characteristics, manufacturing error, or interference issues.

Figure 28. The first (left) and second (right) prototypes of STriDER

6. CONCLUSION

This paper presents a novel rotator joint aligning mechanism for STriDER. Its unique tripedal gait requires three abductor joints to align two of the three body swing rotator joints in the body, depending on the direction of the step the robot takes. Previously the three abductor joints were independently actuated using three DC motors to align the rotator joints which made the robot heavy and inefficient.

In this paper, the synthesis, analysis, and mechanical design of a novel mechanism for actuating the three abductor joints of this unique three-legged walking robot is presented. This mechanism generates the required motion using only a single actuator. It utilizes an internal gear set to generate a Hypotrochoid path curve and uses pin-in-slot joints to coordinate the motion of the three abductor joints to guide them through the four sets of positions required to enable the robot to walk efficiently.

The design constraints and requirements of the abductor joint mechanism were presented along with the synthesis and kinematic analysis of the mechanism which defined the constraints and dimensions used in the force analysis. A study of the force transmission characteristics for a quasi-static case showed several points of infinite mechanical advantage which entailed the mechanism with a unique self-locking ability. Results from early experiments of the robot prototype showed full functionality and confirmed the mathematical analysis.

STriDER's capabilities to walking on uneven ground will be explored which will require the development of 3D dynamic models, unique path planning schemes, and studies on the interaction between STriDER and a variety of environments will be studied next. Work will also be done on incorporating sensors, such as rate gyros and force sensors, to be used for the new controller of the next generation STriDER.

7. ACKNOWLEDGMENT

The authors would like to thank the Office of Naval Research for their support for part of this work under Grant No. N00014-05-1-0828, Nicholas Milo for helping on the fabrication of the prototype, and Mark Showalter who proposed the initial idea for this mechanism.

8. REFERENCES

[1] Hong, D. W., "*Biologically Inspired Locomotion Strategies: Novel Ground Mobile Robots at RoMeLa*", 3rd International Conference on Ubiquitous Robots and Ambient Intelligence, Seoul, S. Korea, October 15-17, 2006.

[2] Heaston, J. R., "*Design of a Novel Tripedal Locomotion Robot and Simulation of a Dynamic Gait for a Single Step*", Masters Thesis, Virginia Polytechnic and State University, 2006.

[3] Heaston, J. R., Hong, D. W., Morazzani, I. M., Ren, P., Goldman, G., "*STriDER: Self-Excited Tripedal Dynamic Experimental Robot*", 2007 IEEE International Conference on Robotics and Automation, Roma, Italy, April 10-14.

[4] Heaston, J. and Hong, D. W., "*Design Optimization of a Novel Tripedal Locomotion Robot Through Simulation and Experiments for a Single Step Dynamic Gait*", 31st ASME Mechanisms and Robotics Conference, Las Vegas, Nevada, September 4-7, 2007.

[5] Ren, P., Morazzani, I. and Hong, D. W., "*Forward and Inverse Displacement Analysis of a Novel Three-Legged Mobile Robot Based on the Kinematics of In-Parallel Manipulators*", 31st ASME Mechanisms and Robotics Conference, Las Vegas, Nevada, September 4-7, 2007.

[6] Spong, M. W. and Bhatia, G., "*Further results on control of the compass gait biped,*" International Conference on Intelligent Robots and Systems, 2003, Las Vegas, Nevada, October 27-30, 2003, pp. 1933-1938.

[7] Lawrence, J. D. A Catalog of Special Plane Curves. New York: Dover, pp. 152-153, 1972.

[8] Uicker. Jr., Pennock, and Shigley, *Theory of Machines and Mechanisms*, 3rd edition. Oxford University Press